Laser-induced forward transfer for printed electronics applications

J. M. Fernández-Pradas[a,c*], P. Sopeña[a,c], S. González-Torres[a,c], J. Arrese[b,c], A. Cirera[b,c], P. Serra[a,c]

[a)] Department of Applied Physics, Universitat de Barcelona, Martí i Franquès 1, 08028, Barcelona, Spain

[b)] MIND, Engineering Department: Electronics, Universitat de Barcelona, Martí i Franquès 1, 08028, Barcelona, Spain

[c)] Institute of Nanoscience and Nanotechnology (IN2UB), Universitat de Barcelona, Joan XXIII S/N, 08028, Barcelona, Spain

* corresponding author: email: jmfernandez@ub.edu
Tel: +34 934039216

Authors ORCID: J.M Fernández-Pradas (0000-0002-9923-1997), A. Cirera (0000-0002-2075-1536), P. Serra (0000-0002-0676-1447)

Abstract

Laser-induced forward transfer (LIFT) is a printing technique based on the action of a laser pulse that is focused on a thin film of a precursor ink for getting the transfer of a droplet onto a receiver substrate. The experiments presented in this article aim to demonstrate the ability of LIFT to produce electronic circuits on paper, a substrate that is flexible, cheap and recyclable. Tests were conducted in order to study the printing of conductive tracks with an Ag ink. The printing of a suspension of carbon nanofibers (CNFs) was also studied in order to demonstrate the ability of LIFT for printing inks with particles with some microns in size that provoke inkjet nozzles to clog. As a proof-of-concept of the LIFT possibilities, both inks were used to print entirely by LIFT a functional humidity sensor on a piece of paper.

All the LIFT experiments were performed with a Nd:YAG laser that delivers pulses of a few hundreds of ns in an attempt to approach the technique to laser systems that are already introduced in many production lines for marking and labeling.

Keywords: Laser-induced forward transfer, printed electronics, paper electronics, sensors

1. Introduction

The idea of using lasers for printing parts of an electronic circuit lies behind some of the first proposals of the laser-induced forward transfer (LIFT) technique [1, 2]. The principle of LIFT is to transfer a small part of material from a thin donor layer onto a receiving substrate under the action of a focused laser beam [3, 4]. Despite being originally considered for transferring patterns from thin solid donor films, the method was extended to the use of liquid films and pastes [5, 6]. In this case, the first applications devised were also in the field of electronics [5].

Printed electronics is gaining increasing interest due to its low cost and possibilities of production on different substrates compared to traditional electronic methods [7]. Thanks to development in this field, electrical devices such as radio frequency identification tags (RFID), solar cells, LEDs, transistors and sensors can be printed on large area and flexible substrates [8, 9]. The extension of electronics to this kind of substrates provides compatibility with roll-to-roll production, with advantages in fast production, cost reduction and easy integration with other technologies.

A very interesting flexible substrate for electronic circuits is cellulose paper [10]. Paper is the cheapest flexible substrate (0.3% of the cost of Kapton®, a typical flexible substrate used in electronics, or 5% of the cost of PET, a very common polymer), and also recyclable, renewable, respectful with the environment, biocompatible, and constantly present in daily life [11, 12]. The printing of RFID devices directly on product labels for tracking and inventory purposes, or the possibility of incorporating electronic circuits on paper money is of clear interest. Furthermore, paper offers the opportunity of integration of both printed electronics and microfluidics in the same substrate in order to produce sensors and point-of-care devices [13, 14].

Screen-printing is the most extended and matured technique for printed electronics [7-9]. However, together with other traditional printing techniques suited for large-scale production like gravure, offset or flexography that are based in the use of masks or moulds, screen-printing does not have the capability to rapidly adapt to changes in the design, causing stops in the production chain [15]. This is one of the reasons why, in an era of rapid changes where customization is a plus, these traditional printing techniques are progressively being substituted by direct-write printing techniques. In this sense, the direct-write ones offer the possibility of printing patterns from a digital file that can be changed at any time, hence making the costs of production independent of the number of runs. Inkjet printing is the most developed direct-write technique [7, 16], and it is well-established in the graphic-arts and labeling industries. However, LIFT has demonstrated

to be able to print a larger range of viscosities [6, 17] than inkjet. Additionally, the absence of nozzle in LIFT avoids clogging issues, and allows printing inks containing particles with sizes up to few hundreds of microns [18]. All these advantages enlarge the number of materials that can be printed and simplify the process of ink formulation. Furthermore, the laser as a tool can be used not only for printing, but also for removing and curing purposes [19]. Thus, LIFT seems a good direct-write alternative to traditional production methods currently used in printed electronics.

The objective of this work is to evaluate the capabilities of LIFT for paper electronics applications. Firstly, the LIFT deposition on paper substrate of a metal conductive ink is systematically studied with the aim to produce conductive electrodes. Conductive inks have been previously printed by LIFT on other substrates [20-27], with some studies especially devoted to produce parts of solar energy devices [28-30]. Secondly, the LIFT of a carbon nanofiber (CNF) suspension on paper was also systematically studied. CNFs are structured materials with good sensing properties that, like nanowires or nanotubes, are difficult to print with inkjet printers as they promote clogging issues of the nozzles. Similar carbon nanostructures have been previously deposited by LIFT from solid donor films [31-33]. In this work, the ink tested is just a suspension of CNFs in water, so the success of printing functional patterns of CNFs by LIFT would demonstrate the easiness of ink preparation and the capability of LIFT for printing inks with long fibers. Finally, as a proof-of-concept, LIFT is used to print all the parts of a humidity sensor device on a piece of paper with both inks. The conductive ink is used to produce the electrodes, and the CNFs are used as sensing material.

2. Experimental

The laser printing system used to perform LIFT was a Nd:YAG laser coupled to a scanner head of galvanometric mirrors (Baasel Lasertech, LBI-6000). The laser operated at the wavelength of 1064 nm delivering pulses at a repetition rate of 1 kHz during all the experiments presented in this work. The energy of the pulses was selected between 50 and 550 μJ by modifying the current of the pumping lamp. The pulse duration using these parameters was around 150 ns. The Gaussian laser beam was focused by an f-theta lens of 100 mm focal length leading to a beam radius of 40 μm at the beam waist. Thus, the average laser fluence (energy density by unit area) ranged from 1.0 to 11 J/cm^2. The scanner head allows to scan the beam up to speeds of 1 m/s in the focal plane. However, all the printing experiments done in this work were performed at a scan speed of 150 mm/s in order to get enough overlap between consecutive pulses for producing continuous lines.

Two different inks were tested in printing experiments that lead to find the parameters for producing a functional gas sensor with them. The first ink is a dispersion of Ag nanoparticles (Sigma Aldrich - 736465) specially formulated for producing conductive patterns on plastic substrates with inkjet printers. The solid content of the ink is around 30-35% with nanoparticles smaller than 50 nm. The ink has a density of 1.45 g/cm^3, a viscosity of 10-18 mPa·s and a surface tension of 35-40 mN/m. The second ink is just a suspension of CNFs in distilled water with a concentration of 20 mg/ml. The CNFs (Grupo Antolin) have a helicoidally graphitic stacked cup structure, a diameter of 20-80 nm, a length of 1-10 μm, a presence of 6% of Ni and a specific surface of 150-200 m^2/cm^3 (Brunauer-Emmet-Teller, N2) [34].

The donor films were prepared by spreading 30 μl of the corresponding ink on a clean microscope glass slide by means of a doctor blade coater. The thickness of the liquid donor layer was around 15 μm. The receiving substrates were sheets of paper (Powercoat HD - Arjowiggins) placed on top of microscope glass slides in order to maximize planarity during the printing process. This paper has a thickness of 230 μm, a density of 220 g/cm^3, and is specially designed for printed electronics applications. The donor layer is placed in front of the receiving substrate surface at a distance of 150 μm and at the focal plane of the f-theta lens.

Before printing, the paper was heated at 150 ^{o}C in an oven during 30 min in order to evaporate impurities. During printing, the receiving substrates were kept at 70 ^{o}C to facilitate the evaporation of the volatile solvents and, hence, to reduce the spreading of the ink on the paper. After printing, all the samples were dried at 55 ^{o}C. Some samples are the result of multiple (2, 4 and 6) printings on the same position. In these cases, the donor layer is refreshed for every time that the laser is scanned again. Before, any new scan, the already printed features were dried and in the case of Ag ink samples, they were heated to 120 ^{o}C. After deposition of all the layers of Ag-ink, the samples were submitted to a curing process for 30 min in an oven at 150 ^{o}C. In the case of the CNF suspension, no curing process was performed after printing.

The morphology of the samples was observed by optical microscopy (Carl Zeiss AX10 Imager.A1) and scanning electron microscopy (SEM, JEOL J-7100). The high roughness of the substrate compared with the thickness of the deposited materials made the measurement of this last by confocal microscopy or stylus profilometry not possible. Resistance of the printed lines was measured with a multimeter (Keithley 175A). With this value and the planar dimensions of the lines, the sheet resistance is then calculated in order to get a parameter independent of the size of the printed features [35].

The humidity sensor was characterized in a customized gas test chamber of 15 ml by sending pulses of gases at different concentrations with a flow of 200 ml/min. The desired humidity level was set by mixing saturated (by bubbling) and dry synthetic air through mass flow controllers. A sequence of four different concentrations was repeated several times. The electrical measurements were performed with a sourcemeter (Keithley 2401). The sensor was not heated during the experiments.

3. Results and discussion

3.1 Printing of Ag ink

The first experiments consisted in the printing of lines of conductive Ag ink at different laser fluences by changing the pulse energy. The lines were 2 cm long. Figure 1 shows optical microscopy and SEM images of the lines. The line width increases with the pulse energy (Figure 2). The line edge roughness (LER) of the printed lines is around 10 μm and does not show any clear trend with pulse energy. The lines appear homogeneous along their cross-sections for laser pulse energies below 380 μJ. When pulse energies above this value are used, the centers of the lines appear darker than the borders. This corresponds to a diminution of the reflectivity, indicating that there is less deposited material in the center than in the border of the lines. This evolution with energy is similar to that found for single droplets deposited on glass substrates with laser pulses of the same duration [27]. Droplets deposited at higher energy were larger, and at the highest energies depletion of material was found in their center. This depletion of material was attributed to the coffee-ring effect [27]. The SEM images show that after the curing process, the deposited lines consisted of grains with 50-100 nm in size (Figure 1). In all the cases, darker zones reveal the presence of porosity. Very few layers of nanoparticles can be seen in the image taken in the center of the line printed at the highest energy (Figure 1f), where even the substrate can be glimpsed. This confirms that less material is deposited in the center of the lines printed at high energy.

When measured, most of the printed lines were shown to be in open circuit (Figure 3). Only the lines printed at 300 and 380 μJ presented a resistance that could be measured with sheet resistance values near 1 kΩ/sq. This denotes lack of continuity in most lines and very thin nanoparticle layers. It must be taken into account that paper is porous, and that its roughness of few microns is much higher than that of other substrates like glass or other polymers used in printed electronics. Thus, the widths of the lines are notably larger than the corresponding diameters of isolated droplets deposited on glass [27]. Owing to the high roughness of the paper, it is not possible to measure the thickness of the printed lines; however, taking into account that isolated droplets on glass have a height below 600

nm, and that droplets spread more on paper, the height of the resulting printed lines is much lower than the substrate roughness. Consequently, lines can easily lose continuity.

In order to get conductive lines, additional layers were deposited by repeating the printing process on the already printed lines, a method that is commonly used for getting conducting lines by inkjet printing [36, 37]. The intention of repeating the printing process is to fill pores and to increase the thickness of the lines. Before every printing process, the previous material was cured at 120 ºC for 30 min. Experiments were conducted by printing lines with 2, 4 and 6 scans. The width of the lines increases as the number of scans increases (Figures 2 and 4). Although this implies a loss of resolution, this is not critical for some applications of paper electronics like sensors or RFID antennas. Nevertheless, resolution can be improved by using smaller laser beam sizes and shorter laser pulses [20-24] or by a later laser ablation step [19]. Measurements of the LER do not show significant variation when increasing the number of scans and its average value continues to be around 10 μm. Images of the lines after several scans show the action of laser pulses in the center of the lines (Figure 4). This effect is especially marked for laser energies above 140 μJ and produces sintering and ablation of part of the material already deposited in previous scans (Figure 4e,f). However, the gain in conductivity justifies the use of multiple scans. With only 2 scans, lines printed with the lowest fluences show sheet resistance values between 20 and 40 Ω/sq (Figure 3). However, some printed lines are open circuit still. After 4 and 6 scans, the lines printed under all the fluences tested show finite resistance. As expected, the sheet resistance diminishes as the number of scans increases. This trend might appear to be easily explained by an increase of the thickness of the lines due to the accumulation of more material. However, the improvement in sheet resistance when comparing 4 and 6 scans is of around one order of magnitude, in contrast with the 6:4 ratio that the thickness could increase, assuming that the same height is added in every new scan. Therefore, an effect of compaction and porosity reduction is also contributing to the sheet resistance decrease. After 6 scans the values of sheet resistance are near or below 1 Ω/sq.

The increasing trend of sheet resistance with increasing values of the pulse energy or fluence could be less intuitive as more material is deposited at higher energies. In a previous work, an even more marked increase of the resistivity of conductive lines with fluence was reported [28]. The hypothesis that a rise in the thermal affected zone could affect the contact resistance is proposed in that case. However, in the case of our work, the morphology of the lines gives a clue for a possible explanation. In one hand, electric current principally circulates by the borders where material is more compact and thicker

for the lines printed at high energy. Consequently, the effective width of these lines is shorter than the real width of the lines. On the other hand, supposing that the morphology of the printed lines has a similar cross-section profile than that of isolated droplets [27], even the border of the lines printed at higher energies would be less thick than the lines printed at low energy. Assuming that resistivity values of the printed material are similar in all cases, lines printed at high energies are thinner than those printed at low energies. As a result, sheet resistance is higher for lines printed at higher energy.

3.2 Printing of C nanofibers ink

The second printing tests were performed with CNFs, a material that presents many restrictions to be printed with inkjet printers due to clogging issues [35]. The solution prepared for LIFT printing is just a suspension of the CNFs in distilled water. This should benefit the sensing properties of CNFs since no additives contaminate the fibers. Figure 5 shows optical microscopy and SEM images of some printed lines. The areas covered by CNFs appear dark in the optical microscopy images. It can be observed that lines printed after 1 or 2 scans are not continuous. In fact, electrical continuity is reached after 4 scans in all cases. The amount of material deposited on the paper increases as the energy rises. The fibers agglomerated in nodules of few microns and preserved their original morphology of high aspect-ratio fibers (Figure 5c,f). The features of the lines are similar to those found in Ag lines: the width of the lines increases as the pulse energy and the number of scans increase. However the lines printed with the CNF suspension are wider than those printed with the Ag ink in all cases. This seems related to the lower viscosity of the CNF suspension in water which is one order of magnitude lower than that of the Ag ink. It has been previously shown that printed droplets spread more with decreasing viscosity under the same laser parameters deposition [17]. In any case, the printing resolution could be improved by using shorter laser pulses and modifying the ink formulation. At high energies more material is concentrated in the border than in the center. This effect, which also occurred in the Ag ink case, could be related to laser ablation of the already deposited material in lines printed through successive scans. However, its occurrence in lines printed with one single scan suggests that, probably, other mechanisms different from the coffee-ring effect can also be involved since some works have shown that large aspect-ratio particles, like CNFs, should notably reduce the coffee-ring effect [38, 39]. Consequently, another mechanism could be responsible here for this higher concentration of material in the borders of lines printed at high energy. This mechanism seems to be related with the different transfer dynamics observed at low and high pulse energies [27]. At low energy, the transfer occurs through the formation of a thin

jet that contacts the receiving substrate, leading to a gentle deposition of the ink that results in the printing of uniform lines. However, the transfer process is completely different at high energy; the generated bubble contacts the receiving substrate before the jet can be formed [27]. In this case, the liquid is transferred much faster (at speeds around 0.1 m/s) and through the walls of the bubble, leading to the deposition of more material in the edges, where the bubble touches the receiving substrate, than in the center.

Electrical characterization of the printed lines after 4 and 6 scans does not show significant differences on the sheet resistance with pulse energy. Lines printed after 4 scans have a sheet resistance near 6 kΩ/sq. After 6 scans the sheet resistance is reduced down to 2kΩ/sq. Thus, after 6 scans the amount of material deposited is enough to ensure both continuity and the sheet resistance value convenient for sensing applications [36].

3.3 Printing and characterization of a humidity sensor

On the basis of the previous results, a functional sensor was entirely printed by LIFT in order to prove the feasibility of the technique in paper electronics applications. First, 8 parallel lines of the Ag ink separated by 600 µm were printed with 140 µJ pulses as interdigitated electrodes. In the same printing process, two wider interconnects were made by overlapping parallel lines (Figure 6a). These elements of the sensor were printed in 6 scans with the same drying, heating and curing steps described in the experimental section during the production of the lines. Electrical characterization of the printed elements showed that the interdigitated electrodes are in open circuit. Afterwards, the CNFs suspension was used to print a square pad of 5 mm×5 mm on the interdigitated electrodes area. The pad of CNFs was deposited by overlapping lines printed also with pulses of 140 µJ, and scanning for 6 times the area with renewed donor layers (Figure 6b). The response of the sensor to cycles of air with different H_2O concentrations is shown in Figure 7. As expected, the response signal increases along the different sequence of pulses, as we found in a previous work for sensors produced on ceramic substrates [40]. Such result is comparable with the response of sensors based in graphene [41]. However, a backfilling issue appears when recovering the sensor with pure synthetic air. This is due to the hydrophilicity of paper and can be solved by heating the sensor [42]. The use of self-heating in 1D structures has proved to manage the power efficiently [40] and to increase the sensor signal quality [43]. However, the use of printing techniques in sensors is limited when lateral resolution becomes a fundamental factor like in FET-based sensors.

4. Conclusion

The results presented in this paper demonstrate the viability of LIFT for printing functional electronic and sensor devices on paper. Conducting tracks can be printed by using inks already formulated for inkjet printing. Sheet resistance values below 1 Ω/sq have been achieved. Furthermore, LIFT easily extends its printing ability to new materials with high technological interest nowadays such as nanofibers, nanotubes or nanowires.

The feasibility of using relatively long laser pulses (150 ns) for printing electronics on paper has been proved. These pulses are common for marking lasers implemented in many factories and would help the reduction of costs, promoting the jump of the LIFT technique from the research laboratory to the productive industry.

Acknowledgement

This work was funded by the AEI of the Spanish Government (Projects TEC2014-54544-C2-1-P and TEC2015-72425-EXP). A. Cirera acknowledges support from the 2015 edition of BBVA Foundation Grants for Researchers and Cultural Creators.

References

[1] A.D. Brisbane, Method for vapour depositing a material in the form of a pattern, Great Britain Patent, GB1,138,084 (1968).

[2] J. Bohandy, B.F. Kim, F.J. Adrian, J. Appl. Phys. 60, 1538 (1986) Metal deposition from a supported metal film using an excimer laser

[3] C.B. Arnold, P. Serra, A. Piqué, MRS Bulletin 32, 23 (2007) Laser direct-write techniques for printing of complex materials

[4] P. Delaporte, A.P. Alloncle, Opt. Laser Technol. 78, 33 (2016) Laser-induced forward transfer: A high resolution additive manufacturing technology

[5] A. Piqué, J. Fitz-Gerald, D.B. Chrisey, R.C.Y. Auyeung, H.D. Wu, S. Lakeou, R.A. McGill, Proc. SPIE 3933, 105 (2000) Direct writing of electronic materials using a new laser assisted transfer/annealing technique

[6] J.M. Fernández-Pradas, C. Florian, F. Caballero-Lucas, P. Sopeña, J.L. Morenza, P. Serra, Appl. Surf. Sci. 418, 559 (2017) Laser-induced forward transfer: Propelling liquids with light

[7] S. Khan, L. Lorenzelli, R.S. Dahiya, IEEE Sensors J. 15, 3164 (2015) Technologies for printing sensors and electronics over large flexible substrates: a review

[8] K. Suganuma, Introduction to Printed Electronics, (Springer, New York , 2014).

[9] R. Venkata Krishna Rao, K. Venkata Abhinav, P.S. Karthik, S. Prakash Singh , RSC Adv. 5, 77760 (2015). Conductive silver inks and their applications in printed and flexible electronics,

[10] Y. Lin, D. Gritsenko, Q. Liu, X. Lu, J. Xu, ACS Appl. Mater. Interfaces 8, 20501 (2016) Recent advancements in functionalized paper-based electronics

[11] D. Tobjörk, R. Österbacka, Adv. Mater. 23, 1935 (2011) Paper electronics

[12] H. Liu, H. Qing, Z. Li, Y.L. Han. M. Lin, H. Yang, A. Li, T. J. Lu, F. Li, F. Xu, Mat. Sci. Eng. R 112, 1 (2017) Paper: A promising material for human-friendly functional wearable electronics

[13] S. K. Mahadeva, K. Walus, B. Stoeber, ACS Appl. Mater. Interfaces 7, 8345 (2015) Paper as a platform for sensing applications and other devices: a review

[14] M.M. Hamedi, A. Ainla, F. Güder, D.C. Christodouleas, M.T. Fernández-Abedul, G.M. Whitesides, Adv. Mater. 28, 5054 (2016) Integrating electronics and microfluidics on paper

[15] J. Rafael Castrejon-Pita, W. R. S. Baxter, J. Morgan, S. Temple, G. D. Martin, I. M. Hutchings, Atomization Sprays 23, 541 (2013) Future, opportunities and challenges of inkjet technologies

[16] B. Derby, Annu. Rev. Mater. Res. 40, 395 (2010) Inkjet printing of functional and structural materials: fluid property requirements, feature stability, and resolution

[17] V. Dinca, A. Patrascioiu, J.M. Fernández-Pradas, J.L. Morenza, P. Serra, Appl. Surf. Sci. 258, 9379 (2012) Influence of solution properties in the laser forward transfer of liquids

[18] G. Hennig, T. Baldermann, C. Nussbaum, M. Rossier, A. Brockelt, L. Schuler, G. Hochstein, J. Laser Micro/Nanoeng., 7, 299 (2012) Lasersonic® LIFT process for large area digital printing

[19] F. Zacharatos, M. Makrygianni, R. Geremia, E. Biver, D. Karnakis, S. Leyder, D. Puerto, P. Delaporte, I. Zergioti, Appl. Surf. Sci. 374, 117 (2016) Laser Direct Write micro-fabrication of large area electronics on flexible substrates

[20] L. Rapp, J. Ailuno, A.P. Alloncle, P. Delaporte, Opt. Express. 19, 21563 (2011) Pulsed-laser printing of silver nanoparticles ink: control of morphological properties

[21] M. Duocastella, H. Kim, P. Serra, A. Piqué, Appl. Phys. A 106, 471 (2012) Optimization of laser printing of nanoparticle suspensions for microelectronic applications

[22] I. Zergioti, J. Laser Micro/Nanoeng. 8, 30 (2013) Laser Printing of Organic Electronics and Sensors

[23] M. Makrygianni, I. Kalpyris, C. Boutopoulos, I. Zergioti, Appl. Surf. Sci. 297, 40 (2014) Laser induced forward transfer of Ag nanoparticles ink deposition and characterization

[24] C. Florian, F. Caballero-Lucas, J.M. Fernández-Pradas, R. Artigas, S. Ogier, D. Karnakis, P. Serra, Appl. Surf. Sci. 336, 304 (2015) Conductive silver ink printing through the laser-induced forward transfer technique

[25] T. Inui, R. Mandamparambil, T. Araki, R. Abbel, H. Koga, M. Nogi, K. Suganuma, RSC Adv. 5, 77942 (2015) Laser-induced forward transfer of high-viscosity silver precursor ink for non-contact printed electronics

[26] C. Florian, F. Caballero-Lucas, J.M. Fernández-Pradas, S. Ogier, L. Winchester, D. Karnakis, R. Geremia, R. Artigas, P. Serra, Appl. Surf. Sci., 374, 265 (2016) Printing of silver conductive lines through laser-induced forward transfer

[27] P. Sopeña, J.M. Fernández-Pradas, P. Serra, Appl. Surf. Sci. 417, 530 (2017) Laser-induced forward transfer of low viscosity inks

[28] M.I. Sanchez-Aniorte, B. Mouhamadou, A.P. Alloncle, T. Sarnet, P. Delaporte, Appl. Phys. A 122, 595 (2016) Laser-induced forward transfer for improving fine-line metallization in photovoltaic applications

[29] D. Munoz-Martina, C.F. Brasz, Y. Chen, M. Morales, C.B. Arnold, C. Molpeceres, Appl. Surf. Sci. 366, 389 (2016) Laser-induced forward transfer of high-viscosity silver pastes.

[30] S. Andree, B. Heidmann, F. Ringleb, K. Eylers, J. Bonse, T. Boeck, M. Schmid, J. Krüger, Appl. Phys. A 123, 670 (2017) Production of precursors for micro-concentrator solar cells by femtosecond laser-induced forward transfer

[31] A. Palla-Papavlu, M. Dinescu, A. Wokaun, T. Lippert, Appl. Phys. A 117, 371 (2014) Laser-induced forward transfer of single-walled carbon nanotubes

[32] C. Constantinescu, S. Vizireanu, V. Ion, G. Aldica, S. D. Stoica, A. Lazea-Stoyanova, A.P. Alloncle, P. Delaporte, G. Dinescub, Appl. Surf. Sci. 374, 49 (2016) Laser-induced forward transfer of carbon nanowalls for softelectrodes fabrication

[33] A. Palla-Papavlu, M. Filipescu, S. Vizireanu, L. Vogt, S. Antohe, M. Dinescu, A. Wokaun, T. Lippert, Appl. Surf. Sci. 374, 312 (2016) Laser-induced forward transfer of hybrid carbon nanostructures

[34] J. Vera-Agullo, H. Varela-Rizo, J.A. Conesa, C. Almansa, C. Merino, I. Martin-Gullon, Carbon 45, 2751 (2007) Evidence for growth mechanism and helix-spiral cone structure of stacked-cup carbon nanofibers

[35] A. Kamyshny, S. Magdassi, Small 10, 3515 (2014) Conductive nanomaterials for printed electronics

[36] T.T. Nge, M. Nogi, K. Suganuma, J. Mater. Chem. C 1, 5235 (2013) Electrical functionality of inkjet-printed silver nanoparticle conductive tracks on nanostructured paper compared with those on plastic substrates

[37] N. Ruecha, O. Chailapakul, K. Suzuki, D. Citterio, Anal. Chem. 89, 10608 (2017) Fully inkjet-printed paper-based potentiometric ion-sensing devices

[38] P.J. Yunker, T. Still, M.A. Lohr, A.G. Yodh, Nature 476, 308 (2011) Suppression of the coffee-ring effect by shape-dependent capillary interactions

[39] X. Wang, G. Kang, B. Seong, I. Chae, H.T. Yudistira, H. Lee, H. Kim, D. Byun, J. Phys. D: Appl. Phys. 50, 455302 (2017) Transparent arrays of silver nanowire rings driven by evaporation of sessile droplets

[40] O. Monereo, J.D. Prades, A. Cirera, Sens. Actuators, B 211, 489 (2015) Self-heating effects in large arrangements of randomly oriented carbon nanofibers: Applications to gas sensors

[41] E. Singh M. Meyyappan, H. S. Nalwa, ACS Appl. Mater. Interfaces 9, 34554 (2017) Flexible Graphene-Based Wearable Gas and Chemical Sensors

[42] S. Claramunt, O. Monereo, M. Boix, R. Leghrib, J.D. Prades, A. Cornet, P. Merino, C. Merino, A. Cirera, Sens. Actuators, B 187, 401 (2013) Flexible gas sensor array with an embedded heater based on metal decorated carbon nanofibres

[43] O. Monereo, O. Casals, J.D. Prades, A. Cirera, Sens. Actuators, B 226, 254 (2016) Self-heating in pulsed mode for signal quality improvement: Application to carbon nanostructured-based sensors.

Figure captions

Figure 1: Optical microscopy images of Ag lines printed by LIFT with pulses of (a) 80, (b) 250, and (c) 550 μJ, after curing. SEM images with details of the Ag lines printed by LIFT with pulses of (d) 80, (e) 250, (f) 550 μJ (g) 550 μJ, after curing. Images in (f) and (g) corresponds to areas in the centre and the border, respectively, of the same line. Scale bar in SEM images corresponds to 1 μm.

Figure 2: Plot of the width of Ag lines printed after 1 (■ black), 2 (● red), 4 (▲ green) and 6 (▼ blue) scans versus the pulse energy. Average fluence is also indicated in the top axis.

Figure 3: Plot of the sheet resistance of Ag lines printed after 1 (■ black), 2 (● red), 4 (▲ green) and 6 (▼ blue) scans versus the pulse energy. Average fluence is also indicated in the top axis.

Figure 4: Optical microscopy images of Ag lines printed by LIFT after 6 scans with pulses of (a) 80, (b) 250, and (c) 550 μJ and after the curing step. SEM images with details of the Ag lines printed by LIFT after 6 scans with pulses of (d) 80, (e) 250, (f) 550 μJ, and after the curing step. Scale bar in SEM images corresponds to 100 nm.

Figure 5: Optical microscopy images of CNF lines printed by LIFT with pulses of 140 μJ and (a) 1 and (b) 6 scans. (c) SEM image with detail of the CNF line in (b). Optical microscopy images of CNF lines printed by LIFT with pulses of 250 μJ and (d) 1 and (e) 6 scans. (f) SEM image with detail of the CNF line in (e). Scale bar in SEM images corresponds to 1 μm. Areas where CNFs were printed appear dark in the optical microscopy images.

Figure 6: Humidity sensor completely printed by LIFT on paper. (a) Interdigitated Ag electrodes and interconnects of the sensor. (b) The complete sensor after printing the CNF pad on the interdigitated electrodes area with soldered wires for response characterization.

Figure 7: Plot of the dynamic response of the humidity sensor printed by LIFT on paper.

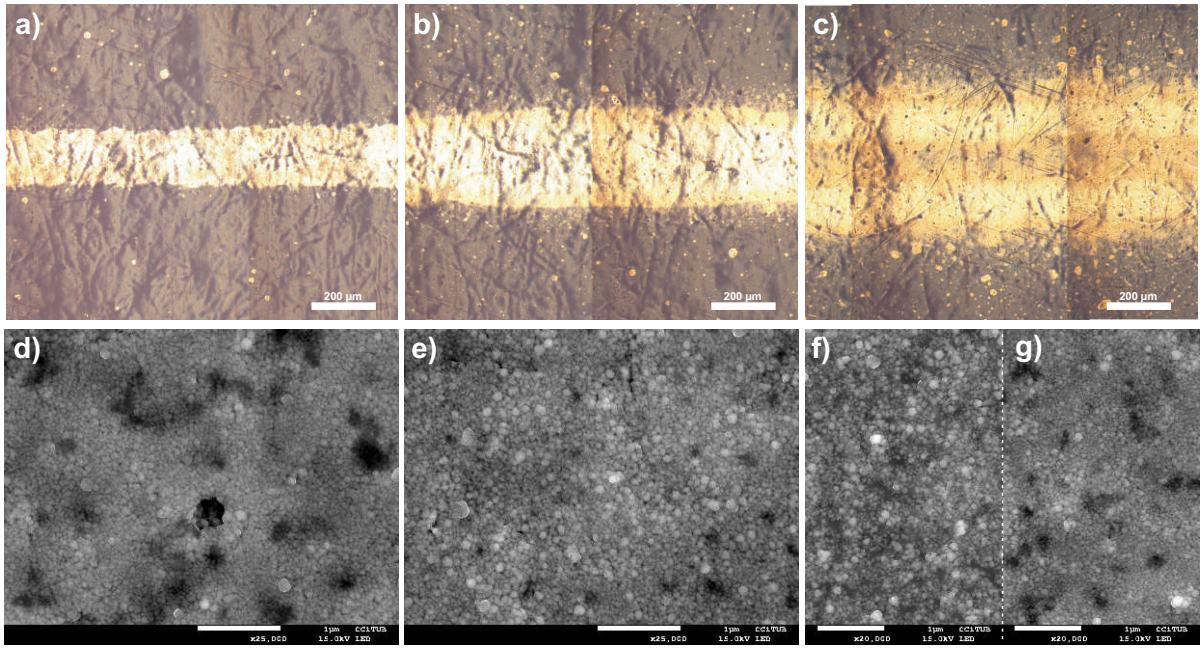

Figure 1

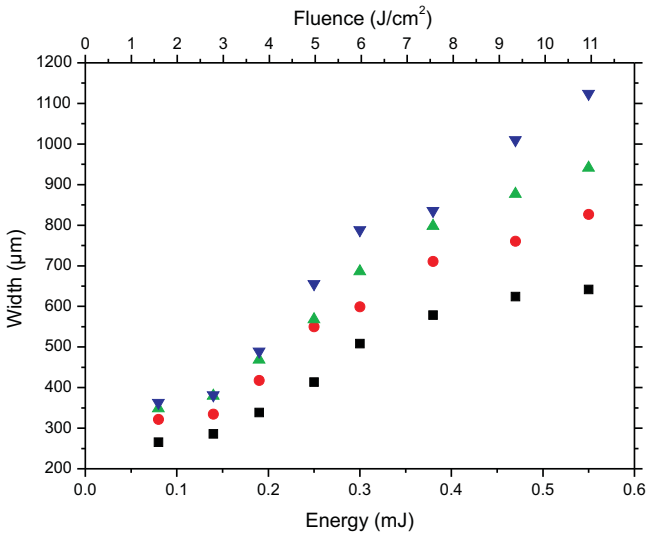
Fluence (J/cm^2)
0
1
2
3
4
5
6
7
8
9
10
11
Width (µm)
1200
1100
1000
900
800
700
600
500
400
300
200
0.0
0.1
0.2
0.3
0.4
0.5
0.6
Energy (mJ)

Figure 2

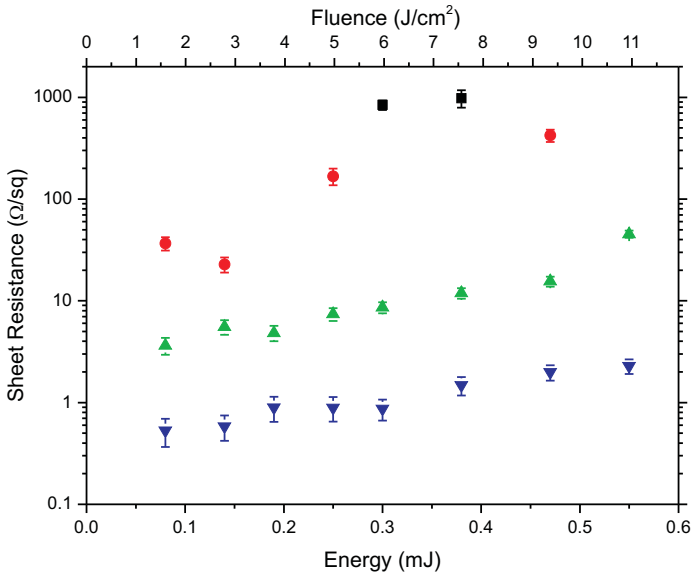
Fluence (J/cm^2)
0
1
2
3
4
5
6
7
8
9
10
11
Sheet Resistance (Ω/sq)
1000
100
10
1
0.1
0.0
0.1
0.2
0.3
0.4
0.5
0.6
Energy (mJ)

Figure 3

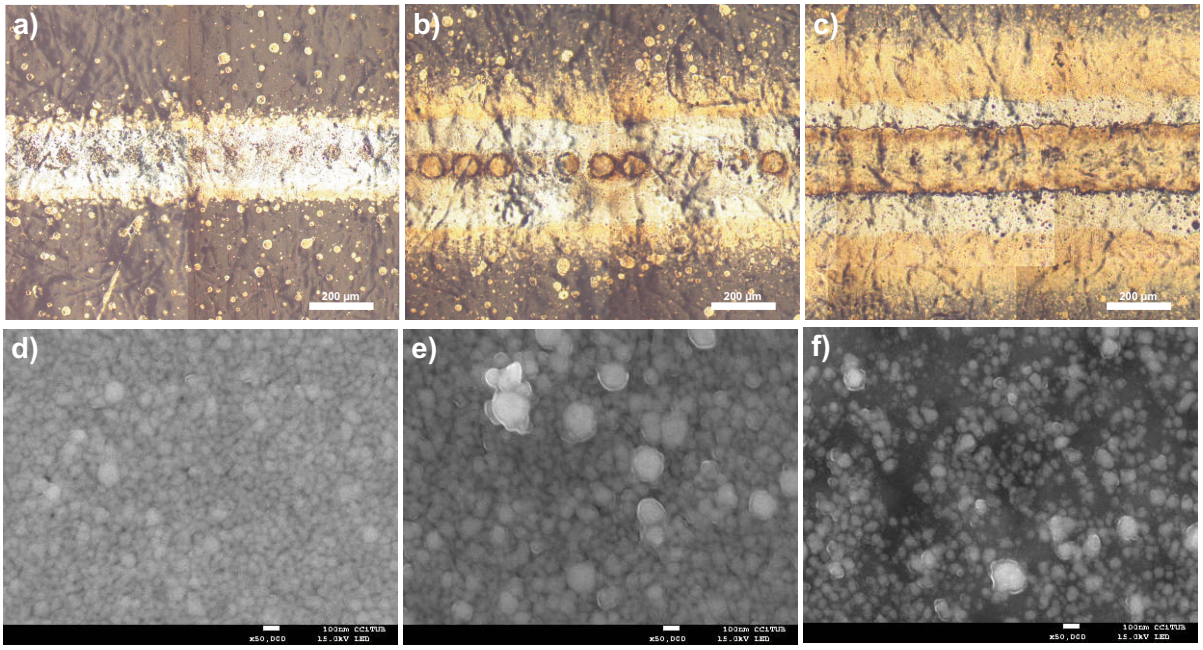

Figure 4

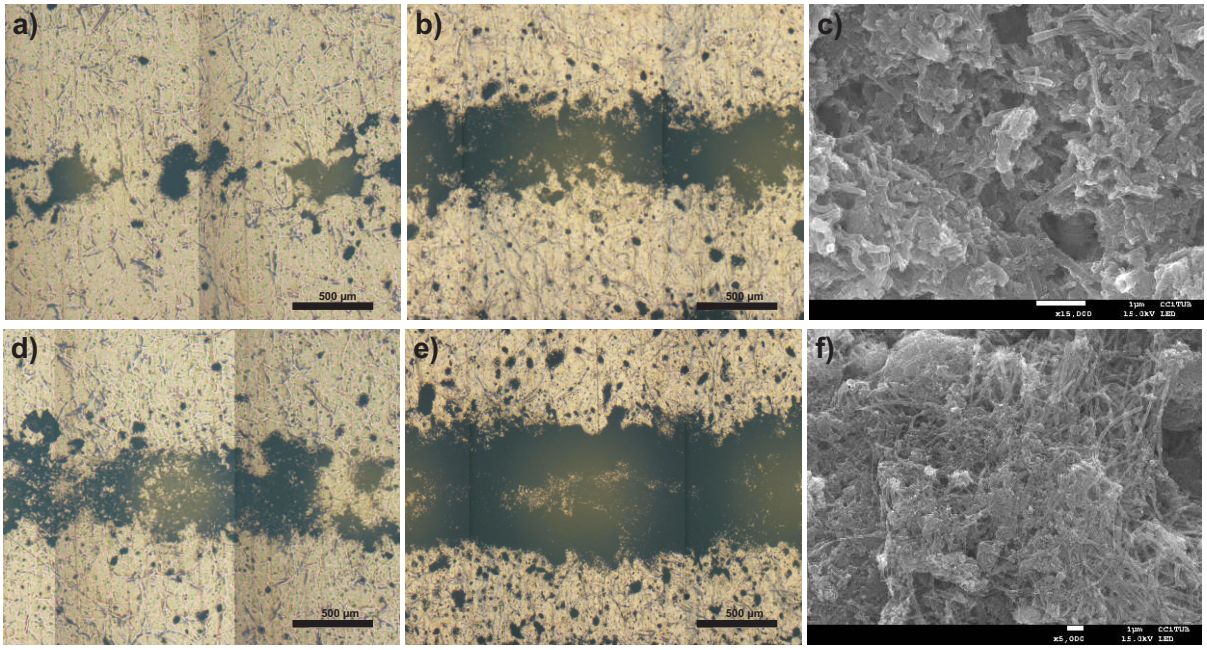

Figure 5

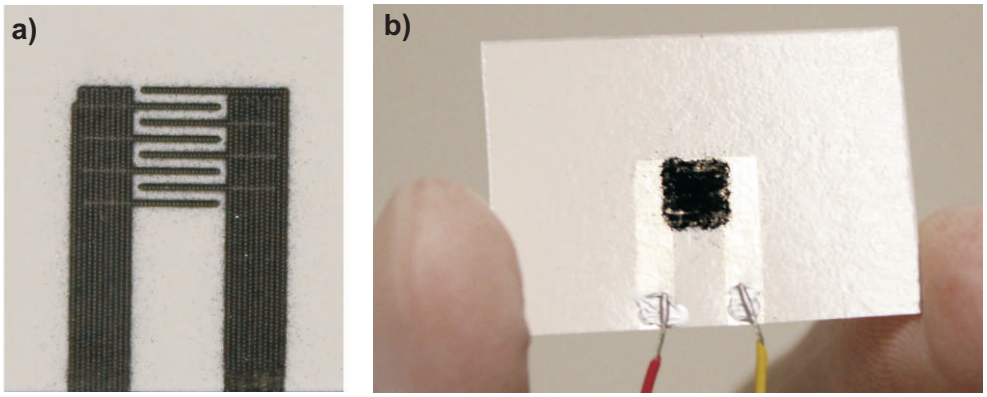

Figure 6

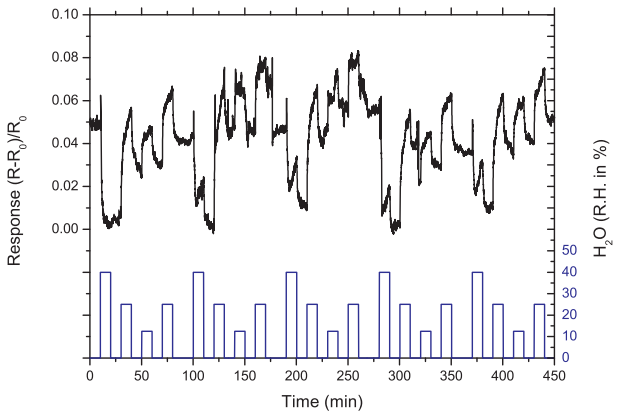
Response (R-R0)/R0
0.10
0.08
0.06
0.04
0.02
0.00
H2O (R.H. in %)
50
40
30
20
10
0
0
50
100
150
200
250
300
350
400
450
Time (min)

Figure 7